Fault Diagnostics with Legacy Power Line Modems

Gautham Prasad*†, Yinjia Huo†, Lutz Lampe†, Anil Mengi*, and Victor C. M. Leung†

*Smart-Grid Strategic Positioning and Innovation, devolo AG, Aachen, Germany.

†Department of Electrical and Computer Engineering, The University of British Columbia, Vancouver, BC.

Email: {gauthamp, yortka, lampe, vleung}@ece.ubc.ca, anil.mengi@devolo.de

Abstract—We evaluate the use of legacy power line modems (PLMs) for fault diagnostics, and in particular, focus on short-circuit faults in underground power cables. Prior works have shown that broadband power line communication channel estimates that are computed within the PLMs can be used to gain insight into the health of underground cables. However, several legacy PLM chip-set implementations do not provide access to the estimated channel frequency response in its entirety. Therefore, to facilitate and accelerate a practical roll-out of a PLM-based diagnostics solution, we investigate if readily extractable parameters, such as the estimated signal-to-noise ratio values and/or the computed precoding matrices in case of multiple-input multiple-output (MIMO) transmission, provide sufficient indication into the cable health status. By extracting suitable features from this raw data, we show through simulations that our machine learning based automated cable diagnostics solution achieves satisfactory results in predicting faults, and near-perfect performance in fault identification.

Index Terms—Smart grid monitoring, fault detection, asset monitoring, machine learning, MIMO-PLC

I. INTRODUCTION

It is estimated that grid faults and the resultant power outages cost an average annual loss of up to \$33 billion in the United States [1]. Proportional values are experienced in other parts of the world as well, e.g., [2], [3]. Apart from financial losses, power outages also lead to potentially hazardous situations and loss of lives [1], [4], [5]. Such scenarios could be caused due to either power line faults, or a component fault, such as a transformer failure [6]. In this paper, we focus on the former as an initial consideration. The solutions we propose, however, are also adaptable for different kinds of faults encountered in the electrical grid.

One class of solutions that addresses the issue of power line faults is a reactive method, where fault localization techniques are designed to identify and locate a fault as quickly as possible to minimize the outage duration [7]–[9]. On the other hand, proactive solutions form another class, where power line faults are predicted in advance to take preventive measures to avoid an eventual in-service failure [10, Ch. 6].

Faults in overhead power lines are predominantly caused by external sources, such as vegetation and other environmental factors, or harsh weather conditions [11], whereas underground cables are known to be resilient to such external factors [12]. Faults are typically experienced in cables when they are subject to prolonged periods of untreated degradation, like thermal, mechanical, or electrical degradation [13]. Hence, fault anticipation in underground wiring infrastructure involves detecting cable anomalies before encountering an in-service failure.

Fault prediction and identification for cables are known to be challenging using conventional diagnostics methods [14], [15]. Additionally, such methods also involve several overheads in terms of cost and effort [16], [17]. All these factors discourage utilities from transitioning toward underground cabling despite its offered benefits, like robustness to weather conditions, reduced impact on the environment, and improved aesthetics of the community [12], [18], [19]. This additionally motivates us to focus on underground cables and investigate cost-efficient and low-effort, i.e., non-destructive, remote, and online, cable diagnostics techniques that can detect and predict cable defects accurately.

Cable health monitoring is not a new field of research, with several solutions having been developed in the past to provide varying extents of diagnostics abilities [10, Ch. 6], [20, Ch. 4]. However, these solutions contain several drawbacks, such as requiring dedicated test equipments or manual waveform analysis for data interpretation [17], [21], which reduce their appeal as they fail to meet the targets we previously outlined. In contrast, a new paradigm of diagnostics techniques was developed recently, where solutions were designed to reuse power line modems (PLMs) that are installed throughout the neighborhood area network (distribution network) for smart-grid communications, to also monitor the cable health status [22]–[27]. These methods involve inspecting changes in the communication channel state information (CSI), which is inherently estimated within the PLMs, to infer a deviation in the power cable health, either manually [22], [23], or automatically using machine learning (ML) techniques [24]–[27]. While such solutions are able to achieve all our set targets, the demand for extracting the estimated power line communication (PLC) CSI introduces practical challenges. Popular chip-sets used within broadband PLC (BB-PLC) modems, such as [28], do not provide external access to the estimated CSI in its entirety. Instead, companion firmwares can only extract other channel-related parameters, such as the estimated signal-to-noise ratio (SNR) values and the computed precoding matrix in case of multiple-input multiple-output (MIMO) PLC [29]. In this paper, we present an investigation to determine if these parameters provide useful insights into the status of the cable health so that native implementation of the existing chip-sets need not be altered to accommodate the additional cable diagnostics functionality.
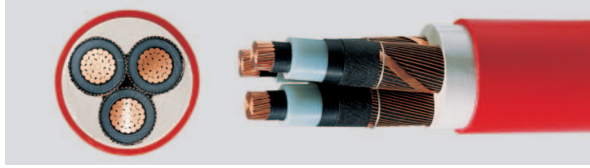
Fig. 1. The triple-core XLPE-insulated N2XSEY cable that we consider for our evaluations [32].

Intuitively, we expect that the diagnostics performance using the computed precoding matrix would be degraded as opposed to using the entire CSI, since the precoding matrix does not necessarily retain all information contained in the channel frequency response [30, Ch. 8]. With this backdrop, we begin by examining the performance of cable fault detection using the precoding matrix computed for MIMO transmit beamforming. We then evaluate the types of faults and degradations that can be detected and assessed using the computed precoding matrices.

Similar to the loss of information faced by using precoding matrices, using SNR values also introduces the drawback that their changes are influenced not only by variations in channel conditions but also by power line noise. Furthermore, although MIMO transmission is supported in new-generation smart-grid PLC products [31], we wish to examine the compatibility of our solution to operate with SISO modems. To this end, we also investigate the diagnostics performance in detecting cable anomalies solely using SNR values.

We show through simulations that our ML-based diagnostics technique achieves near-ideal results in detecting the presence of low-impedance line-to-line and line-line-line faults using either of the two extractable parameters, while the detection accuracy using SNR suffers when the insulation breakdown is incomplete, i.e., when a degradation has not sustained long enough to cause an eventual low-impedance fault.

II. FAULT DIAGNOSTICS

In this section, we provide the preliminaries of the applied PLC channel and fault modeling procedures and MIMO beamforming technique used, and proceed to detail our proposed diagnostics methods.

A. PLC Channel Model

We apply the bottom-up approach to model PLC channels to accurately capture the effects of cable faults. While a top-down channel modeling procedure may be computationally simpler, the bottom-up approach allows us to locally describe a range of faults and determine its impact on the channel.

Channel generation using the bottom-up approach requires knowledge about the power line network topology, loads connected at each of the end points, and the power cable description, including its length and per-unit-length (PUL) parameters to capture the conductor and insulation types of the cable and its physical cross sectional dimensions.

1) Cable Characterization: For an n-core cable, we compute the PUL parameters matrices, i.e., the $(n-1) \times (n-1)$ order resistance ($\mathbf{R}$), inductance ($\mathbf{L}$), capacitance ($\mathbf{C}$), and
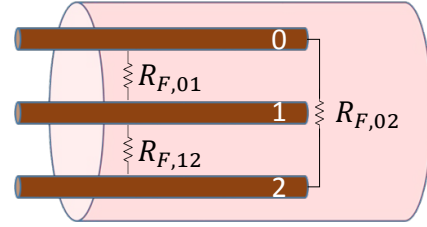

Fig. 2. Conceptual representation of short-circuit faults in triple-core underground cables.

conductance ($\mathbf{G}$) matrices, at any frequency f, with the 0th conductor as reference using [33, Ch. 3, Ch. 5]

$$R_{ij} = R_0 + R_j, \qquad i = j, \qquad (1)$$

$$R_{ij} = R_0, \qquad i \neq j, \qquad (2)$$

$$L_{ij} = \frac{\mu_0}{2\pi} \ln\left(\frac{d_{0,j}^2}{r_0 r_j}\right), \qquad i = j, \qquad (3)$$

$$L_{ij} = \frac{\mu_0}{2\pi} \ln\left(\frac{d_{0,i} d_{0,j}}{r_0 d_{i,j}}\right), \qquad i \neq j, \qquad (4)$$

$$\mathbf{C} = \mu_0 \epsilon_0 \Re(\epsilon_{\mathsf{ins}}) \mathbf{L}^{-1} \qquad (5)$$

$$\mathbf{G} = -2\pi f \mu_0 \epsilon_0 \Im(\epsilon_{\mathsf{ins}}) \mathbf{L}^{-1}, \qquad (6)$$

where $0 \leq (i,j) \leq n-1$, R_j is the PUL resistance of the jth conductor, R_{ij} and L_{ij} are the (i,j)th elements of $\mathbf{R}$ and $\mathbf{L}$, respectively, $d_{i,j}$ is the separation between the ith and the jth conductor, r_j is the radius of the jth conductor, μ_0 and ϵ_0 are the free-space permeability and permittivity, respectively, and ϵ_{ins} is the complex permittivity of the cable insulation [24, Table 1]. In this work, we consider a 500 m long triple-copper-core cable with cross-linked polyethylene (XLPE) insulation shown in Fig. 1, with $\epsilon_{\mathsf{ins}} = 2.3 - 0.001\sqrt{-1}$, $d_{0,1} = d_{0,2} = d_{1,2} = 15.8$ mm and $r_0 = r_1 = r_2 = 3.99$ mm [32].

2) Network Characterization: As an initial investigation, we consider a simple cable segment with no branches in between. Such a radial topology, however, is not uncommon in medium voltage networks where BB-PLC repeaters are installed approximately every $400 - 800$ m [34]. To emulate realistic network extensions beyond the two ends of the cable, we connect randomized loads at both ends in parallel with the PLMs, where the loads are chosen from $\left(\mathscr{U}(0,50) + \sqrt{-1}\,\mathscr{U}(-50,50)\right)$ Ω [30, Table 1.1], with $\mathscr{U}(a,b)$ indicating a uniform random distribution between a and b.

B. Fault Modeling

We now introduce faults in the healthy cable models that we derived. Faults be classified into low- and high-impedance ones. For multi-core cables, such as the one we consider, insulation breakdown caused due to, say, sustained degradation like water-treeing, results in low-impedance short-circuit faults. We model this condition by introducing a fault impedance load, $R_{F,ij}$, between the ith and the jth conductors, as shown in Fig. 2. Further, faults can either occur in an asymmetric or symmetric/balanced fashion. When symmetric short-circuit

faults occur in triple-core cables, two or more fault impedances are shorted, while asymmetric faults can be characterized by a negligibly small $R_{F,ij} \approx 0 \ \Omega$ for only one of the three fault impedances. The individual values of $R_{F,ij}$ can also be varied to emulate a diverse set of cable faults and insulation damages, which we explore in Section III.

C. Parameters for Monitoring

As alluded to in Section I, we use the two readily extractable parameters from the PLMs, namely, the precoding matrix and the SNR values, for cable health monitoring. In the following discussion, we introduce the beamforming procedure applied in MIMO-PLC to understand the impact of channel variations on the estimated precoding matrix, and also analyze the impact of faults on the SNR, which is the only extractable channel-dependent raw data from legacy modems in SISO operation.

1) Beamforming in MIMO-PLC: Spatial multiplexing for MIMO transmission in PLC is obtained by transmitting different data streams over the available transmit ports. Depending on the beamforming technique applied, the transmitter computes the precoding matrix using the estimated CSI.

We represent the MIMO channel matrix as $\mathbf{H}(f)$, given by

$$\mathbf{H}(f) = \begin{bmatrix} h_{11}(f) & h_{12}(f) & ... & h_{1N_{\mathsf{TX}}}(f) \\ h_{21}(f) & h_{22}(f) & ... & h_{2N_{\mathsf{TX}}}(f) \\ \vdots & \vdots & \ddots & \vdots \\ h_{N_{\mathsf{RX}}1}(f) & h_{N_{\mathsf{RX}}2}(f) & ... & h_{N_{\mathsf{RX}}N_{\mathsf{TX}}}(f) \end{bmatrix}, \quad (7)$$

where $h_{k\ell}(f)$ is the complex channel transfer function (CTF) between the ℓth receiver and the kth transmitter at any frequency f, and N_{TX} and N_{RX} are the number of active transmit and receive ports used, respectively. MIMO PLMs typically implement *Eigen-beamforming* over the active transmit ports [35]. Accordingly, the precoding matrix, $\mathbf{F}$ is the right-singular unitary matrix, $\mathbf{V}$, which can be obtained by the singular value decomposition of $\mathbf{H}$ [30, Ch. 8], i.e.,

$$\mathbf{H}(f) = \mathbf{U}(f)\mathbf{D}(f)\mathbf{V}^{H}(f), \quad (8)$$

where $\mathbf{D}$ is a diagonal matrix of order $\min(N_{\mathsf{TX}}, N_{\mathsf{RX}})$, $\mathbf{U}$ is the left-hand unitary matrix, and $(\cdot)^{H}$ is the conjugate transpose operator. We notice from (8) that using $\mathbf{V}(f)$ in place of $\mathbf{H}(f)$ could produce differing diagnostics results. Hence, we investigate through simulations presented in Section III, if $\mathbf{V}(f)$ contains sufficient information to provide satisfactory fault diagnostics performance.

2) SNR for SISO Operation: Since $\mathbf{V}$ is unavailable when the PLM operates in the SISO mode, we also study the impact of faults on the estimated SNR values. The SNR, ρ, can be computed as

$$\rho(f) = \frac{P_{\mathsf{TX}}(f) \cdot |h(f)|^2}{N_{\mathsf{PLC}}(f)}, \quad (9)$$

where $P_{\mathsf{TX}}(f)$ is the transmit power spectral density, $h(f)$ is the complex SISO CTF, and $N_{\mathsf{PLC}}(f)$ is the cumulative power line noise power spectral density at the receiver. We readily notice two disadvantages with using $\rho(f)$ in place of $h(f)$. First, in addition to $h(f)$, the changes in $\rho(f)$ are also affected by $N_{\mathsf{PLC}}(f)$. Therefore, it is harder to train a machine to instantaneously recognize changes in $\rho(f)$ that are caused due to a fault. Furthermore, since $\rho(f)$ is only dependent on the attenuation of the channel, we lose its phase information, which is essential to gain knowledge of the presence and locations of signal peaks in the channel impulse response that are caused due to a cable fault.

D. ML for Fault Diagnostics

Following the discussion in Sections II-B and II-C, we note that a cable fault changes the overall network impedance, and therefore also causes a change in $\mathbf{H}(f)$ and consequently in $\mathbf{V}(f)$ and $\rho(f)$. We use supervised ML techniques to intelligently distinguish changes caused due to cable faults and other network activities, like load variations, based on individual observations of $\mathbf{V}$ and ρ. To this end, we borrow the underlying ML diagnostics framework from our previous works in [25], [27].

We formulate the fault identification task as an ML classification problem, and use the adaptive boosting (*AdaBoost*) algorithm to train our machine. Being one of the meta-ML algorithms that consolidates multiple weak learners into a strong learner, AdaBoost is known to be robust to over-fitting and can be efficiently executed since it is a forward stage-wise additive model [36, Ch. 16]. The performance of AdaBoost is dependent on the quality of the used features that are extracted from the raw data, i.e., $\mathbf{V}$ or ρ. Using prior works that have used ML for cable diagnostics [24], [26], we determine that the mth order moments ($m = 1, 2, 3, 4$) of ρ or $v_{k\ell}$, i.e., the (k, ℓ)th element of $\mathbf{V}$, provide insight into the change in cable health as a result of the additional frequency dependent attenuation introduced by cable anomalies. However, we show in Section III that these features are inadequate to obtain satisfactory results, and we thus extract additional ones from $\mathbf{V}$ and ρ to obtain greater insight into cable faults. As an alternative to this feature engineering task, one could also use automated ML (AutoML) tools, which can automatically select the most suitable ML algorithm(s) and also perform the necessary data preprocessing for machine training [37]. An evaluation of one such AutoML tool, called Auto-SKLearn, for cable diagnostics can be found in [38].

III. EVALUATION

In the following, we present a simulation evaluation of our proposed ML-based diagnostics design. To prepare the machine for testing, we train it with different samples, i.e., channel conditions, including healthy and faulty cables that are subject to both symmetric and asymmetric faults. We choose the number of training samples such that the performance of the ML algorithm is saturated at its highest level [27, Appendix. B]. For our considered task, we choose 7000 training samples. Further, to obtain a clear performance trend we use 1000 different testing samples for evaluation. We generate PLC channels using an open-source channel emulator tool under varied network load conditions [39]. To build faulty cables, we randomly place low-impedance cable faults
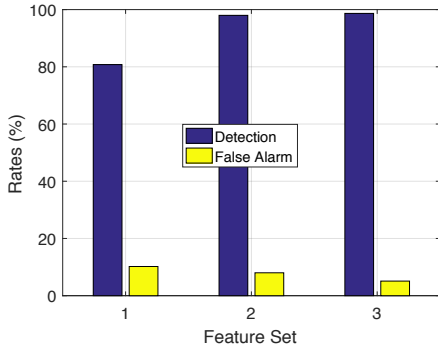
Fig. 3. Detection and false alarm rates for identifying symmetric L-L-L cable faults using different feature sets.
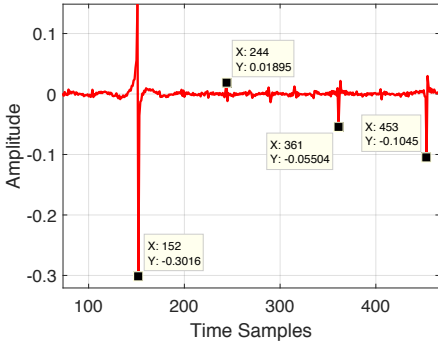

Fig. 5. Detection and false alarm rates for identifying asymmetric line-to-line cable faults using different feature sets.

Fig. 4. Inverse Fourier transform of v_{12} with a short-circuit cable fault at $d_F = 348$ m, where data pointers indicate the signal peak positions caused by the direct and reflected paths.

Fig. 6. Variation of detection and false alarm rates with changing fault impedances using features extracted from $\mathbf{V}$.

at different distances, d_F, from the transmitting PLM at one end of the cable.

A. Fault Diagnostics using Precoding Matrix

We begin our investigations by considering a 2×2 MIMO-PLC system, where signals are coupled and decoupled between the conductor pairs $0-1$ and $0-2$ on each end (refer Fig. 2). We then use $\mathbf{V}$ as the raw data from which we extract features for ML training and testing.

1) Performance under Different Types of Faults: We first examine the detection and false alarm rates that we obtain for detecting symmetric faults using $\mathbf{V}$. To this end, we set the fault impedance $R_{F,01} = R_{F,12} = R_{F,02} = 1$ Ω for a faulty cable to emulate a line-line-line (L-L-L) fault. The results of this exercise are shown in Fig. 3, where the variation of detection and false alarm rates are provided for different feature sets used in the ML operation. Feature Set 1 consists of the primitive set of features described in Section II-D, i.e., the mth order moments ($m = 1, 2, 3, 4$) of $v_{k\ell}$ across frequency. We notice that this results in unsatisfactory detection rates of about 80% and over 1 in 10 cases of false alarms. Therefore, to improve the results, we study the inverse Fourier transform of $v_{k\ell}$ for each of $k, \ell \in \{1, 2\}$. Fig. 4 shows a window of the time domain version of v_{12}, where we observe four strong signal peak locations corresponding to the four prominent receptions of the direct and the reflected signals that we would observe in the channel impulse response. Hence, we add the signal peak locations and amplitudes in Feature Sets 2 and 3,
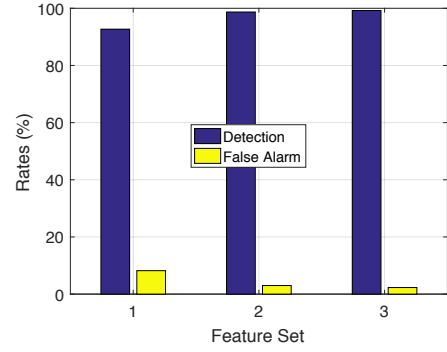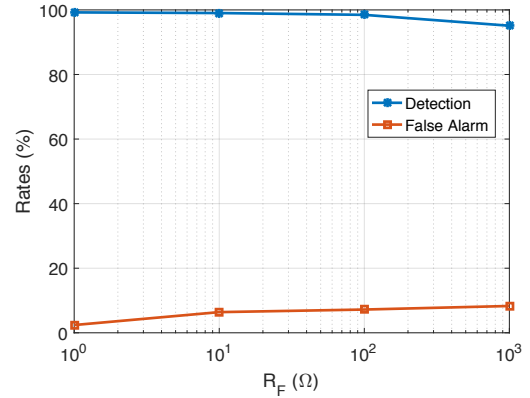
respectively. This improves the detection rates to 98.7% and reduces the false alarm by half by using Feature Set 3, as seen in Fig. 3.

Fig. 5 presents similar results for asymmetric faults, which we generate by setting $R_{F,ij} = 1$ Ω for randomly chosen $i, j \in \{0, 1, 2\}$ with $i \neq j$. We notice that we continue to obtain comparable results with up to 99.2% detection rate using Feature Set 3, and a false alarm of 2.3%. Henceforth, we restrict our evaluations to asymmetric faults as we expect to encounter more of these over their symmetric counterparts.

2) Performance under Different Fault Impedances: We have thus far evaluated the performance of our solution to detect the presence of near-ideal faults where $R_{F,ij} = 1$ Ω. In the following, we investigate the performance when the characteristics of the fault deviate from this ideal behavior. Furthermore, increasing $R_{F,ij}$ also approximates an insulation breakdown that is not complete, i.e., it emulates partial damage of the insulation[1], which when left untreated could result in an eventual short-circuit fault. We present these results in Fig. 6 obtained using Feature Set 3, where we notice that, despite the performance reduction with increase in $R_{F,ij}$, we still obtain over 95% detection rates and a false alarm rate

---

[1]Note that a frequency-flat resistive fault does not always accurately model insulation degradation, which could present a frequency selective impedance [24]. However, our evaluation focuses only on estimating the potential of using $\mathbf{V}$ for cable degradation diagnostics.
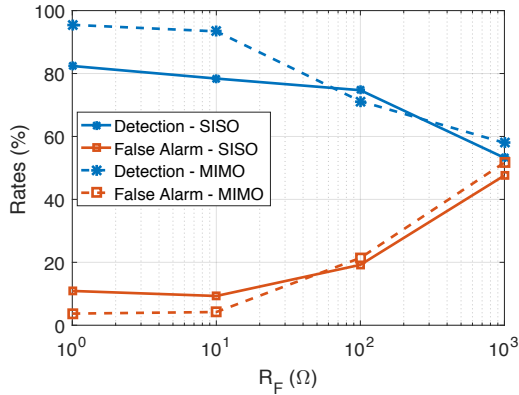
Fig. 7. Variation of detection and false alarm rates with changing fault impedances using features extracted from SNR values under SISO and MIMO communication scenarios.

of 8.3% even at $R_{F,ij} = 1$ kΩ. This signifies the potential of using $\mathbf{V}$ for also detecting *soft* faults, such as early-stage insulation degradations, indicating that our solution can also be effectively applied for fault prediction.

B. Fault Detection using SNR Values

To determine the applicability of our solution on SISO-PLMs, we investigate its performance using ρ as the raw data that are extracted from SISO-PLMs transmitting and receiving data between the $0 - 1$ conductor pair. We compute ρ using Eq. (9) with $P_{\mathsf{TX}}(f) = -50$ dBm/Hz across all frequencies in accordance with the North American regulations [40, Ch. 3], [41], and N_{PLC} randomly determined with the 'worst-case' setting in the cumulative power line noise generator of [42]. The results of using ρ for fault diagnostics are shown in Fig. 7. We notice that when the insulation breakdown is prominent, that is, at low $R_{F,ij}$ values, we detect over 8 out of 10 faults. However, as $R_{F,ij}$ increases, the detection and false alarm rates deteriorate. For comparison, we also show the diagnostics results we obtain by using the SNR values from MIMO-PLC modems, which can be used for diagnostics under conditions where $\mathbf{V}$ is unavailable for use. Although we notice more accurate performance at lower values of $R_{F,ij}$ in this case, both detection and false alarm rates deteriorate with increase in fault impedance values. This shows that while the machine is able to detect cable faults using SNR, subtle changes caused by insulation degradations are harder to distinguish in the presence of power line noise.

IV. DISCUSSION

In this section, we present a brief discussion by suggesting practical implementation approaches and critically analyzing our proposed solution.

A. Applicability Across PLC Technologies

Our evaluations focused on using BB-PLC channel transfer functions for fault detection and prediction. However, our solution is also applicable for fault diagnostics using narrowband PLC (NB-PLC) CSI. While the outlined diagnostics procedure remains the same, the behavior deviations in the CTFs between

intact and faulty cables at low frequencies would drive the features that need to be extracted from the raw data for decision making. An initial investigation in this regard was performed in [25], where it was shown that extracting ML features from channel frequency responses in the narrow bandwidth at low frequencies provides comparable results to BB-PLC for long run cables. This suits the application scenarios of NB-PLC, which is typically used to obtain extended transmission range at the cost of lower data rate and higher response times.

B. Off-Site Analysis

Our solution builds on existing ML- and PLC-based diagnostics techniques that propose loading one or more trained machines onto existing PLMs in the grid through software/firmware upgrades, such that these PLMs can independently and automatically diagnose cable defects. However, storing machines and performing ML tasks through feature extraction within the PLMs introduce additional storage requirements and increase in computational complexity, respectively. To counter this drawback, we propose an alternative implementation architecture, where the raw data (BB-PLC CSI) is collected from all PLMs at a central location, either at secondary sub-stations or the central office of the utilities. Data processing, including feature extraction and decision making can then performed at the central location. This further reduces modifications required within legacy PLM implementations to accommodate the grid diagnostics functionality. Furthermore, such an implementation also simplifies the ML update mechanism since it does not require any PLM firmware upgrades to use an improved ML algorithm in the future, and is also not limited by the computational ability or resources available within the PLM. As a result, we believe that it outweighs the additional communications overhead that this architecture may introduce.

C. Fault Location and Degradation Severity Prediction

The peak locations observed in Fig. 4 indicates that $\mathbf{V}$ can be used not only to detect the presence of a cable fault, but also for fault location. By integrating ML operation, we can formulate this task as a regression problem, and boosting techniques like least-squares boosting can be applied to estimate the location of the fault. Furthermore, as the fault impedance varies, the peak amplitudes seen in Fig. 4 also vary due to the change in impedance mismatch conditions. Therefore, $\mathbf{V}$ also provides insight into the extent of insulation degradation, in addition to detecting and locating those anomalies. Similar exercises have been shown to be successful in the past, in the context of assessing localized water-tree cable degradations, using $\mathbf{H}$ [27].

D. Performance Verification Under Practical Conditions

Further to designing techniques that require minimal changes to legacy PLMs, practical deployment of our solution involves the final step of evaluating its performance under real-world conditions. This includes our ongoing work of laboratory measurements to validate the simulation models we

use, and also field trials with commercial PLMs to capture the effects of power line noise during channel estimation that could impact the results in Section III.

V. CONCLUSION

We have presented a machine learning based diagnostics solution to reuse legacy power line modems for cable fault detection and prediction. By analyzing the computed precoding matrix and the estimated SNR values that are available to be extracted from the existing modems, we have proposed methods to detect the presence of symmetric and asymmetric faults in underground power cables. Our simulation results show that we obtain up to 99.2% and 82% detection rates in fault identification using legacy MIMO- and SISO-PLC modems, respectively. As a result, our method demands no changes to native chip-set implementations and functions as a true add-on feature with the existing modems, which accelerates the practical deployment of a PLC-based grid diagnostics solution.

REFERENCES

[1] "Economic benefits of increasing electric grid resilience to weather outages," *Washington, DC: Executive Office of the President*, 2013.

[2] J. Reichl, M. Schmidthaler, and F. Schneider, "The value of supply security: The costs of power outages to Austrian households, firms and the public sector," *Energy Economics*, vol. 36, pp. 256–261, 2013.

[3] Blackout tracker: Canada annual report 2014. [Online]. Available: http://pqlit.eaton.com/ll_download_bylitcode.asp?doc_id=24003

[4] A. Castillo, "Risk analysis and management in power outage and restoration: A literature survey," *Electric Power Systems Research*, vol. 107, pp. 9–15, 2014.

[5] F. J. Shields, "The problem of arcing faults in low-voltage power distribution systems," *IEEE Trans. Ind. Appl.*, vol. IGA-3, no. 1, pp. 15–25, 1967.

[6] D. D. Shipp, T. J. Dionise, V. Lorch, and B. G. MacFarlane, "Transformer failure due to circuit-breaker-induced switching transients," *IEEE Trans. Ind. Applicat.*, vol. 47, no. 2, pp. 707–718, March 2011.

[7] J. A. Jiang, C. L. Chuang, Y. C. Wang, C. H. Hung, J. Y. Wang, C. H. Lee, and Y. T. Hsiao, "A hybrid framework for fault detection, classification, and location—part I: Concept, structure, and methodology," *IEEE Trans. Power Del.*, vol. 26, no. 3, pp. 1988–1998, 2011.

[8] "IEEE guide for determining fault location on AC transmission and distribution lines," *IEEE Std C37.114-2014 (Revision of IEEE Std C37.114-2004)*, pp. 1–76, Jan 2015.

[9] M. Jamei, A. Scaglione, and S. Peisert, "Low-resolution fault localization using phasor measurement units with community detection," in *IEEE Int. Conf. on Commun. Control and Computing Tech. Smart Grid (SmartGridComm)*, 2018, pp. 1 – 6.

[10] P. Gill, *Electrical power equipment maintenance and testing*. CRC press, 2008.

[11] L. Wang, "The fault causes of overhead lines in distribution network," in *MATEC Web of Conferences*, vol. 61. EDP Sciences, 2016, pp. 1–5.

[12] H. Orton, "History of underground power cables," *IEEE Electr. Insul. Mag.*, vol. 29, no. 4, pp. 52–57, 2013.

[13] J. Densley, "Ageing mechanisms and diagnostics for power cables - an overview," *IEEE Electr. Insul. Mag.*, vol. 17, no. 1, pp. 14–22, 2001.

[14] L. A. Griffiths, R. Parakh, C. Furse, and B. Baker, "The invisible fray: A critical analysis of the use of reflectometry for fray location," *IEEE Sensors Journal*, vol. 6, no. 3, pp. 697–706, 2006.

[15] A. Cozza and L. Pichon, "Echo response of faults in transmission lines: Models and limitations to fault detection," *IEEE Trans.s on Microwave Theory and Techniques*, vol. 64, no. 12, pp. 4155–4164, 2016.

[16] P. Wang, M. R. Raghuveer, W. McDermid, and J. C. Bromley, "A digital technique for the on-line measurement of dissipation factor and capacitance," *IEEE Trans. Dielectr. Electr. Insul.*, vol. 8, no. 2, pp. 228–232, 2001.

[17] V. Dubickas, "On-line time domain reflectometry diagnostics of medium voltage XLPE power cables," Ph.D. dissertation, KTH, 2006.

[18] P. Fairley, "Utilities bury more transmission lines to prevent storm damage," *IEEE Spectr.*, vol. 2, pp. 9–10, 2018.

[19] Head to head - overhead vs underground. [Online]. Available: https://westernpower.com.au/community/news-opinion/head-to-head-overhead-vs-underground/

[20] P. B. Andersen, E. B. Hauksson, A. B. Pedersen, D. Gantenbein, B. Jansen, C. A. Andersen, and J. Dall, *Smart grid applications, communications, and security*. Wiley, 2012.

[21] J. Wang, P. Stone, Y.-J. Shin, and R. Dougal, "Application of joint time–frequency domain reflectometry for electric power cable diagnostics," *IET Sig. Processing*, vol. 4, no. 4, pp. 395–405, 2010.

[22] F. Passerini and A. M. Tonello, "Full duplex power line communication modems for network sensing," in *IEEE Int. Conf. on Smart Grid Commun. (SmartGridComm)*, 2017, pp. 1 – 5.

[23] A. M. Lehmann, K. Raab, F. Gruber, E. Fischer, R. Müller, and J. B. Huber, "A diagnostic method for power line networks by channel estimation of PLC devices," in *IEEE Int. Conf. on Smart Grid Commun. (SmartGridComm)*, 2016, pp. 320–325.

[24] Y. Huo, G. Prasad, L. Atanackovic, L. Lampe, and V. C. M. Leung, "Grid surveillance and diagnostics using power line communications," in *Proc. IEEE Int. Symp. Power Line Commun. Appl. (ISPLC)*, 2018, pp. 1–6.

[25] Y. Huo, G. Prasad, L. Lampe, and V. C. M. Leung, "Cable health monitoring in distribution networks using power line communications," in *IEEE Int. Conf. on Commun. Control and Computing Tech. Smart Grid (SmartGridComm)*, 2018, pp. 1 – 6.

[26] L. Förstel and L. Lampe, "Grid diagnostics: Monitoring cable aging using power line transmission," in *Proc. IEEE Int. Symp. Power Line Commun. Appl. (ISPLC)*, 2017, pp. 1–6.

[27] Y. Huo, G. Prasad, L. Lampe, and V. C. M. Leung, "Cable diagnostics with power line modems for smart grid monitoring," *arXiv preprint arXiv:1808.01149*, 2018.

[28] QCA7500 Chipset. [Online]. Available: https://www.qualcomm.com/products/qca7500

[29] "dLAN Software Development Kit," *Devolo AG*. [Online]. Available: https://bit.ly/2E24OR7

[30] L. T. Berger, A. Schwager, P. Pagani, and D. Schneider, *MIMO power line communications: narrow and broadband standards, EMC, and advanced processing*. CRC Press, 2014.

[31] "Five reasons for broadband powerline in the intelligent measuring system," *Broadband Powerline for the roll-out*, 2018. [Online]. Available: https://goo.gl/WZAN5y

[32] HELUKABEL. Medium voltage power cables. [Online]. Available: https://bit.ly/2rfoppb

[33] C. R. Paul, *Analysis of multiconductor transmission lines*. John Wiley & Sons, 2008.

[34] devolo. BPL modem MV: Data communication at the medium voltage level. [Online]. Available: https://bit.ly/2E3n1Oj

[35] L. Yonge, J. Abad, K. Afkhamie *et al.*, "An overview of the HomePlug AV2 technology," *J. of Elec. and Comp. Eng.*, 2013.

[36] K. Murphy, *Machine Learning: A Probabilistic Perspective*, ser. Adaptive computation and machine learning. MIT Press, 2012.

[37] M. Feurer, A. Klein, K. Eggensperger, J. Springenberg, M. Blum, and F. Hutter, "Efficient and robust automated machine learning," in *Advances in Neural Information Processing Systems*, 2015, pp. 2962–2970.

[38] Y. Huo, G. Prasad, L. Lampe, and V. C. M. Leung, "Smart-grid monitoring: Enhanced machine learning for cable diagnostics," in *IEEE Int. Symp. Power Line Commun. Appl. (ISPLC)*, 2019.

[39] F. Gruber and L. Lampe, "On PLC channel emulation via transmission line theory," in *Proc. IEEE Int. Symp. Power Line Commun. Appl. (ISPLC)*, 2015, pp. 178–183.

[40] L. Lampe, A. M. Tonello, and T. G. Swart, *Power Line Communications: Principles, Standards and Applications from Multimedia to Smart Grid*. John Wiley & Sons, 2016.

[41] FCC-Part15, "Radio frequency devices," *FCC, USA*, 2003.

[42] G. Prasad, H. Ma, M. J. Rahman, F. Aalamifar, and L. Lampe. A cumulative power line noise generator. [Online]. Available: http://www.ece.ubc.ca/~gauthamp/PLCnoise